

# Entropy-Based Multirobot Active SLAM

Muhammad Farhan Ahmed<sup>a,\*</sup>, Matteo Maragliano<sup>b</sup>, Vincent Frémont<sup>a</sup>, Carmine Tommaso Recchiuto<sup>b</sup>

<sup>a</sup>Laboratoire des Sciences du Numérique de Nantes (LS2N), CNRS, Ecole Centrale de Nantes, 1 Rue de la Noë, 44300, Nantes, France

<sup>b</sup>University of Genoa, 5 Via Balbi, 16126, Genova, Italy

---

## Abstract

In this article, we present an efficient multi-robot active SLAM framework that involves a frontier-sharing method for maximum exploration of an unknown environment. It encourages the robots to spread into the environment while weighting the goal frontiers with the pose graph SLAM uncertainty and path entropy. Our approach works on a limited number of frontier points and weights the goal frontiers with a utility function that encapsulates both the SLAM and map uncertainties, thus providing an efficient and not computationally expensive solution. Our approach has been tested on publicly available simulation environments and on real robots. An accumulative 31% more coverage than similar state-of-the-art approaches has been obtained, proving the capability of our approach for efficient environment exploration.

**Keywords:** SLAM, Active SLAM, Frontier Detection, Mapping, Entropy

---

## 1. Introduction

Simultaneous localization and mapping (SLAM) is an approach where an agent autonomously localizes itself and simultaneously maps the environment while navigating through it. The objective is to find the optimal state vector that minimizes the measurement error between the estimated pose and environmental landmarks. Most SLAM algorithms are passive, i.e., the robot is controlled manually and the navigation or path planning algorithm does not actively take part in robot motion or trajectory. Active SLAM (A-SLAM), however, tries to solve the optimal exploration problem of the unknown environment by proposing a navigation strategy that generates future goal/target positions actions which decrease map and pose uncertainties, thus enabling a fully autonomous navigation and mapping SLAM system without the need of an external controller or human effort.

In Active Collaborative SLAM (AC-SLAM) multiple robots interchange information to improve their localization estimation and map accuracy to achieve some high-level tasks such as exploration. The exchanged information can be localization information [1], entropy [2], visual features [3], and frontier points [4]. In this article, we present a multi-agent AC-SLAM system for efficient environment exploration using frontiers detected over an Occupancy Grid (OG) map. In particular, in this work, we aim at:

1. Extending the A-SLAM approach of [5] which uses a computationally inexpensive D-optimality criterion for utility computation to a multi-agent AC-SLAM framework.
2. Proposing a utility function that uses frontier path entropy for computing the rewards of goal candidate frontiers.
3. Introducing a method that coordinates the frontiers sharing among robots to encourage maximum distance between robots for exploration.
4. Implementing the proposed method in ROS using both simulation and real robot experiments and achieving an accumulative 31% more coverage than state-of-the-art methods.

---

\*Corresponding author

Email addresses: Muhammad.Ahmed@ec-nantes.fr (Muhammad Farhan Ahmed), 4636216@studenti.unige.it (Matteo Maragliano), vincent.fremont@ec-nantes.fr (Vincent Frémont), carmine.recchiuto@dibris.unige.it (Carmine Tommaso Recchiuto)

The proposed system aims to efficiently maximize the environment exploration while maintaining good SLAM estimates and provides a not computationally expensive solution by reducing the number of goal frontiers.

The article is organized as follows: Section 2 summarises the related literature from selected articles. Section 3 presents a thorough explanation of our proposed system, with specific emphasis on the methodologies employed for frontier filtering and management, implementation of the utility function, and coordination among robots. We show the usefulness and application of the system in simulations and real robot experiments in Sections 4.1 and 4.2. Finally, in Section 5 we summarize and conclude this work. Throughout this article, we will use the words *robots* or *agents* interchangeably, and the same applies to *frontiers* and *points*, as they imply the same meaning in the context.

## 2. Related Work

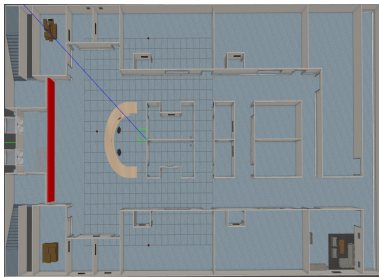
As previously mentioned, A-SLAM is designed for situations in which a robot must navigate in an environment that is only partially observable or unknown. In this context, the robot must choose a sequence of future actions while dealing with noisy sensor measurements that impact its understanding of both its state and the map of the environment. This scenario is typically formalized as a specific case of the Partially Observable Markov Decision Process (POMDP), as presented in [24], [17], and [19].

The POMDP formulation of A-SLAM, while widely adopted, is computationally intensive to streamline computation, A-SLAM is usually divided into three key steps: 1) identifying potential goal positions (frontiers, i.e., boundaries between visited and unexplored areas), 2) calculating their associated costs using a utility function where utility is computed using Information Theory (IT) [10] or Theory of Optimal Experimental Design (TOED) [11], hence selecting the next action to be performed, and 3) executing the action, eventually moving the robot to the chosen goal position.

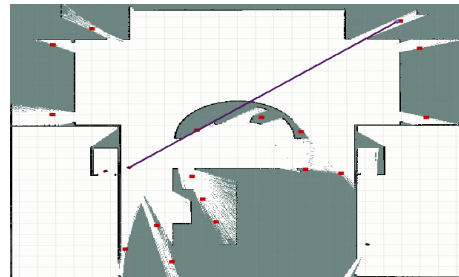
Concerning the first step, a common approach consists of letting the robot identify potential exploration targets using the frontier-based approach pioneered by Yamauchi [6]. Figure 1 illustrates frontier detection using lidar measurements within a simulated AWS Modified Hospital environment<sup>1</sup>.

To manage exploration, IT strategies are based on the use of information as a measure of utility for taking exploration control actions. As the uncertainties related to the map and robot pose increase over time, the goal is to reduce the uncertainties in the belief space [21] about the unknown environments. The existing approaches propose solutions that make use of particle filters [2][7], Mutual Information [8] [9], Bayesian Optimization [9], and entropy [2]. In IT, entropy measures the amount of uncertainty associated with a random variable or random quantity. Higher entropy leads to less information gain and vice versa. The authors in [2] formulate the Shannon entropy of the Map  $M$  as in Equation 1 where the map is represented as an occupancy grid and each cell  $m_{i,j}$  is associated with a Bernoulli distribution  $P(m_{i,j})$ . The objective is to reduce both the robot pose and map entropy.

$$\mathcal{H}[p(M)] = - \sum_{i,j} (p(m_{i,j}) \log(p(m_{i,j})) + (1 - p(m_{i,j})) \log(1 - p(m_{i,j}))) \quad (1)$$



(a) Simulated environment



(b) Computed occupancy grid map and frontiers detection

Figure 1: (1a) AWS Modified Hospital environment. (1b) Frontier detection on the occupancy grid map, red = robot, green = detected frontiers (centroids), white = free space, gray = unknown map area, black = obstacles

<sup>1</sup><https://github.com/mlherd/>

Alternatively, TOED defines many “optimality criteria”, which give a mapping of the covariance matrix to a scalar value. Hence, the priority of a set of actions is based on the amount of covariance in the joint posterior. Less covariance contributes to a higher weight of the action set. The “optimality criterion” deals with the minimization of average variance, minimizing the volume of the covariance ellipsoid (D-optimality), and minimization of the maximum eigenvalue [13].

Many of the concepts previously discussed can be found even in the case of Active Collaborative SLAM (AC-SLAM) with the additional constraint of managing inter-robot robust communications. Typical application scenarios include collaborative localization [18][22], exploration and exploitation tasks [26][26] and trajectory planning [15][16].

In detail, multi-agent frontier-based strategies assess information gain and detect frontiers through interactions, as seen in [28] and in wireless sensing networks [30]. The method described by [26] formulates the problem in an environment represented by primitive geometric shapes. The cost function is somewhat similar to [27], which takes into consideration the discovery of the target area of a robot by another member of the swarm and switches from a frontier to a distance-based navigation function to guide the robot toward the goal frontier.

Other research works have implemented frontiers-based coverage approaches that divide the perception task into a broad exploration layer and a detailed mapping layer, making use of heterogeneous robots to carry out the two tasks [3] while solving a Fixed Start Open Traveling Salesman Problem (FSOTSP) for frontier-based viewpoints has been proven as a valid solution to build a volumetric model of the environment with multiple agents [4].

With a similar approach, the authors in [27] and [1] describe frontier-based exploration as an optimization problem where the information gain and localization efficiency (measured as a trace of the covariance matrix) is maximized while navigation cost towards the frontier is penalized.

More recently another method for quantifying uncertainty, based on the graph connectivity indices underlying the pose graph SLAM structure, has emerged as a valid approach in the AC-SLAM scenario. Graph connectivity indices are computationally less expensive to measure SLAM uncertainty as compared to TOED and IT approaches discussed previously. In [22], the authors propose a method for identifying weak connections in pose graphs to strategically enhance information exchange when robots are in proximity. In other words, the proposed system identifies the weak connections in the target robot pose-graph, and when the covariance increases to a certain threshold, other agents help to rectify these weak connections and generate trajectories using Rapidly Exploring Random Trees (RRT) [20] to decrease uncertainty and improve localization. This method uses continuous refinement along with the D-optimally criterion to collaboratively plan trajectories. A bidding strategy is defined, which selects the winning host robot based on the least computational cost, feasible trajectory, and resource-friendly criteria.

### 3. Methodology

#### 3.1. Overview of the proposed approach

Overall, the AC-SLAM approaches discussed in Section 2 quantify the uncertainty using the entire map entropy and by using the full covariance matrix which renders them computationally expensive. Further, they do not favour the spread of agents for maximum coverage requirements. For these reasons, here we propose an AC-SLAM method that encourages sparsity between agents while utilizing a utility function that takes into account the uncertain propagation not only of the pose-graph (D-optimality) but also of the map (frontier path). Indeed, using our approach we manage to spread the agents while maintaining a good SLAM estimate. Also, when compared to the state-of-the-art methods described in Section 2 our method provides a computationally efficient solution by working on fewer frontiers, maximizing the exploration while using a utility function incorporating modern D-Optimality along with path entropy.

Figure 2 shows the architecture and communication pipeline of our proposed approach. We have built our method upon [5] which uses a Lidar-based SLAM back-end and proposes a utility function based on the D-Optimality criterion as a maximum number of spanning trees of the graph Laplacian of the pose-graph. Each robot performs its SLAM using Open Karto <sup>2</sup> and detects local frontiers regarding its map. A map merging node <sup>3</sup> (map-merging-node) merges

<sup>2</sup>[https://github.com/ros-perception/slam\\_karto](https://github.com/ros-perception/slam_karto).

<sup>3</sup><https://github.com/robo-friends/m-explore-ros2>

local maps into a global map, so that all the computed frontiers are referenced to the global map. Frontiers from each agent are concatenated into a list and further processed by the Filtering and Classification (*merge-points-server*) module (Section 3.2). This module removes redundant frontiers and further filters the frontiers/points by keeping only those points that are at (or near to) the border of the merged map (global map). This new list of points is given back to each agent which computes its utility and reward matrix for each point as we will see in the Utility Computation (*assigner* node) module (Section 3.3). This reward matrix is further processed by the Update Rewards & Goal Selection (*choose-goals-server*) module (Section 3.4) which updates the rewards keeping into account the sparsity and number of already selected goal points for each agent. Finally, the selected goal for each agent is sent to the Path planning & control module (ROS Navigation stack) which uses Dijkstra’s algorithm [12] for global and Dynamic Window Approach (DWA) [33] as local planners.

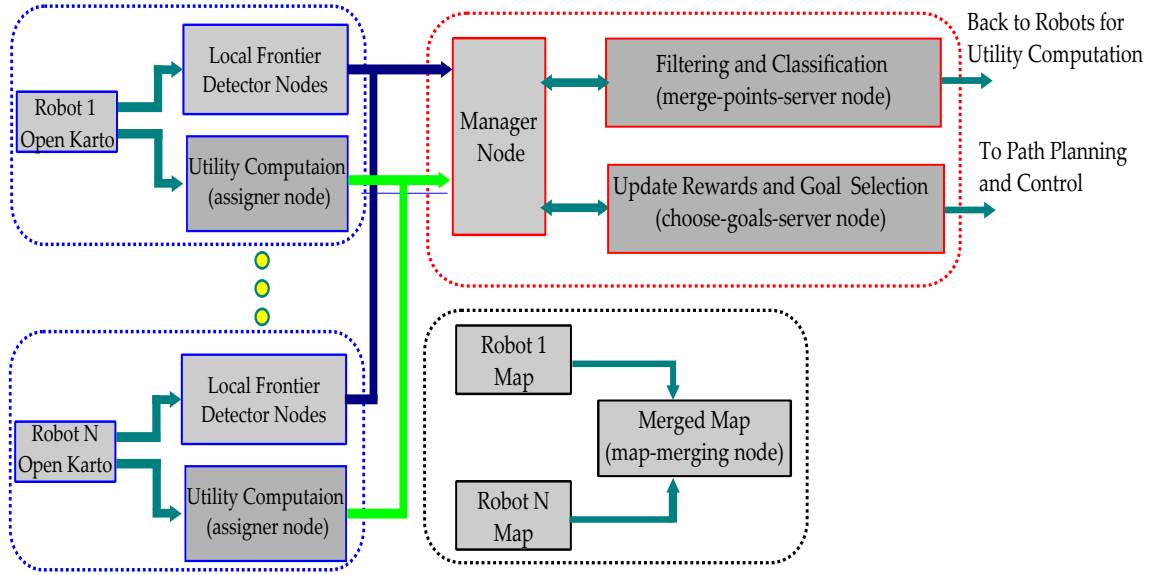


Figure 2: Architecture of the proposed method. Local nodes of each robot (blue), ROS server (red), map-merging mode (black)

Since the approach has been implemented in ROS and involves a centralized frontiers sharing system as shown in Figure 2 each agent uses two main nodes responsible for utility computation and frontier detection: the *assigner* node computes the proposed utility function and assigns the goal points to the agent, while the *detector* nodes use OpenCV and RRT-based frontier detection from [5]. The following nodes are a part of the *central server* of the system: 1) the *map-manager* node, responsible for the communication among the entire server and each agent in the system, 2) the *merge-points-server* node, responsible for merging lists of points acquired by different agents, and 3) the *choose-goals-server* node, which chooses a specific target point in the list. By adopting a specific policy (Section 3.4), the server also tries to distribute the robots in the environment and reduce the exploration time.

Concerning following Sections and Algorithms, we can summarize the workflow as:

1. Each agent detects the points  $p$  and passes them to the central server (subject to its availability) on a dedicated topic.
2. The manager node takes the list of points  $p_{list}$  passed by the agents and sends it to *merge-points-server*.
3. The *merge-points-server* takes as input the lists received by all robots, merging the points into a unique list using Algorithm 1, also checking the actual frontiers on the merged map  $M$  through the Algorithm 2 and limiting the dimension of the list using the procedure explained in Algorithm 3. Eventually, it gives back the list to each agent.
4. Each agent computes the reward matrix  $R_m$  on the received list, with the approach described in Section 3.4, sending it to the *choose-goals-server*.
5. The *choose-goals-server* server updates the reward through Algorithms 4 and 5 to take into account all the points already assigned. The selected target point is fed back to the robot.

6. The global and local planners of the ROS package *move\_base* are responsible for driving each agent to the selected frontier. Once the agent reaches the target, the workflow restarts from step 1.

In the following Sections, we describe comprehensively steps 3, 4, and 5, which represent the core of the proposed approach.

### 3.2. Filtering and classification

Each agent is responsible for building its map and merging local frontier points as shown in Algorithm 1. Some parts of the map from each agent can be overlapped and the frontiers could lie in an already mapped area when considering the merged map. Since usually the goal of an exploration task is to cover the entire area by minimizing the exploration time, the frontiers lying in the middle of the merged map are not significant because moving an agent to them would not increase the overall discovered area.

To avoid the need to consider these points as *goal-like* points, we decided to filter the points considering only the actual frontiers of the merged map. To this purpose, Algorithm 1 takes a list of points  $P_{list}$  and the merged map  $M$  and it checks if each point has enough unknown cells (PRC\_UNK) around it, in a radius (RAD) (line 3), i.e., if the point is near the border. If so, the point is added to the global list  $uni_{pts}$ . This process (line 3) of Algorithm 1 is detailed in Algorithm 2. In particular, it may be observed how the percentage PER\_UNK of unknown cells (Line 18) contained in the radius RAD is used to discriminate whether to keep a point in the list or not (Line 19).

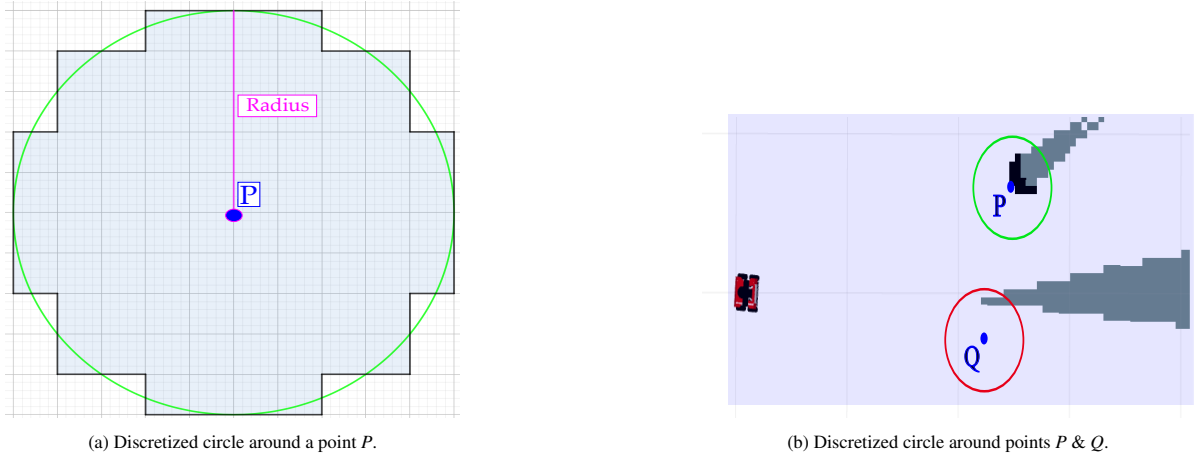


Figure 3: General 3a and Occupancy Grid Map Representation 3b of the Discretized circle

---

#### Algorithm 1 Merge Points

---

**Require:**  $p_{list}, M$

$\triangleright p_{list} = \{x_1, y_1, \dots, x_N, y_N\}, \text{merged\_map} = M$

**Ensure:**

```

1:  $uni_{pts} \leftarrow 0$ 
2: for  $p \in p_{list}$  do
3:   if  $N_{bdr}(p, M, RAD, PRC\_UNK)$  then
4:     if  $p \notin uni_{pts}$  then
5:        $uni_{pts} \leftarrow p$ 
6:     end if
7:   end if
8: end for

```

$\triangleright$  add  $p$  to unique list of points

---

To provide an example of this approach, Figure 3b shows an example list of two points  $P$  and  $Q$  in a partially discovered map. The Algorithm 1 in conjunction with Algorithm 2 identifies, for both points, a circle as shown in Figure 3a and computes the percentage of the unknown cells over the total one contained inside the circle. Once the

---

**Algorithm 2** Check if a Point is Near the Map Border
 

---

```

1: function  $N_{bdr}(p, M, rad, \text{PRC\_UNK})$ 
2:    $c_x \leftarrow (p_x - M_{origx})/M_{res}$ 
3:    $c_y \leftarrow (p_y - M_{origy})/M_{res}$ 
4:    $Rad_c \leftarrow rad/M_{res}$ 
5:    $Cir_c \leftarrow \{\}, unk_{cnt}, tot_c \leftarrow 0$ 
6:   for  $i, j \in Rad_c$  do
7:      $cel_i \leftarrow c_x + i, cel_j \leftarrow c_y + j$ 
8:     if  $cel_i, cel_j \geq 0$  &
        $< M_w, M_h$  then
9:        $idx \leftarrow cel_i + cel_j \times M_{width}$ 
10:       $Cir_c \leftarrow cel_i, cel_j$ 
11:      if  $M_{data}[idx] = -1$  then
12:         $unk_{cnt} \leftarrow unk_{cnt} + 1$ 
13:      end if
14:       $tot_{cells} \leftarrow tot_{cells} + 1$ 
15:    end if
16:  end for
17:  if  $tot_{cells} \neq 0$  then
18:     $unk_{perc} \leftarrow \left( \frac{unk_{cnt}}{tot_{cells}} \right) \times 100$ 
19:    if  $unk_{perc} \geq \text{PRC\_UNK}$  then
20:      return True
21:    end if
22:  end if
23:  return False
24: end function

```

---



---

**Algorithm 3** Check list dimension
 

---

**Require:**  $p_{list}, M, rad, \text{PRC\_UNK}$   
**Ensure:**

```

1: while  $uni_{pts} \leq \text{MIN\_PTS}$  or
    $\geq \text{NUM\_PTS}$  do
2:   if  $uni_{pts} \leq \text{MIN\_PTS}$  then
3:      $uni_{ptsN} \leftarrow \text{list}, uni_{pts} \leftarrow \{\}$ 
4:      $perc = perc - 10$ 
5:     for  $p \in uni_{ptsN}$  do
6:       if  $N_{bdr}(p, M, rad, \text{PRC\_UNK})$  then
7:         if  $p \notin uni_{pts}$  then
8:            $uni_{pts} \leftarrow p$ 
9:         end if
10:      end if
11:    end for
12:  else if  $uni_{pts} \geq \text{NUM\_PTS}$  then
13:     $uni_{ptsN} \leftarrow uni_{pts}$ 
14:     $uni_{pts} \leftarrow \{\}$ 
15:     $rad = rad + 0.25$ 
16:    for  $p \in uni_{ptsN}$  do
17:      if  $N_{bdr}(p, M, rad, \text{PRC\_UNK})$  then
18:        if  $p \notin uni_{pts}$  then
19:           $uni_{pts} \leftarrow p$ 
20:        end if
21:      end if
22:    end for
23:  end if
24: end while

```

---

percentage is computed, this point is kept or discarded based on the threshold of PER\_UNK set during the program execution. In the specific case, opportunely setting PER\_UNK, point  $P$  will be added to the global list, i.e., considered as a border point, whereas point  $Q$  will be discarded.

Even discarding points that are not on the border, having many agents may lead to having extensive lists of points that need to be processed; to avoid this problem, we decided to bind the number of points to process using Algorithm 3. After the list is created, there is another check to validate the boundaries of the list dimension as described in Algorithm 3. Concerning this algorithm, if the list has fewer points than the minimum required (i.e., MIN\_PTS), the same is recomputed by decreasing the threshold PER\_UNK used in Algorithm 2 by 10% as shown in Line 4. On the other hand, if the list has more points than a maximum threshold NUM\_PTS, the list is reprocessed by increasing the radius RAD (Algorithm 2) by 0.25m (Line 15 of Algorithm 3).

### 3.3. Utility computation

Once the global list of frontier points is created, it is sent to the *assigner* node of each agent for the computation of the utility function for each frontier candidate, by applying the Bresenham's line algorithm [34] to get the occupancy values of all the pixels within the straight path from the agent to the frontier location. For computing the Entropy, we assign a probability value equal to  $P_{unknown} = 0.1$  to the occupancy values of unknown pixels, to quantify low entropy and high information gain (as we are more interested in unknown areas of the environment). Occupancy values of obstacles and free space are mapped with a probability  $P_{known} = 0.45$ , quantifying high entropy and low information gain.

Using these probability values and Equation 1, the path entropy  $E$  for each frontier candidate is computed. The path entropy is then normalized with the number of pixels/cells within the frontier path  $L$ . We apply an exponential decay operator  $\gamma = \exp^{-(\lambda * dist)}$  with decay factor  $\lambda = 0.6$  (kept constant as we assume static environment) and Euclidean distance  $dist$  for penalizing frontiers with large distances. Finally, the proposed utility  $U_2$  as shown in Equation 2 is computed by weighing normalized entropy with  $\rho = 10^\beta$ , where  $\beta$  is a factor which depends on the number of spanning trees of the weighted graph Laplacian  $L_w$  computed in Equation 3 and adopted from [5]. More explicitly  $\beta$  is the the number of digits before the decimal places of  $U_1$  and acts as a balancing factor between entropy and the number of spanning trees.

Eventually, we obtain the proposed utility function  $U$  in Equation 4, which not only provides a good SLAM estimate based on the modern D-Optimality criterion but also increases the coverage of the unknown map by reducing the frontier path entropy.

$$U_2 = (1 - E/L) * \rho + \gamma \quad (2)$$

$$U_1 = \text{Spann}(L_w) \quad (3)$$

$$\text{Reward} = U = \max(U_1 + U_2) \quad (4)$$

The Reward  $r_{0:N}$  is assigned through the matrix  $R_m$  for each agent, as shown in Equation 5, where  $N$  is the number of points detected.

$$R_m = \begin{bmatrix} \text{Reward} & X & Y \\ r_0 & x_0 & y_0 \\ r_1 & x_1 & y_1 \\ \vdots & \vdots & \vdots \\ r_N & x_N & y_N \end{bmatrix} \quad (5)$$

### 3.4. Update Rewards and Goal selection

Once each agent has computed its reward matrix, each matrix is sent to the *choose-goals-server* (hereafter referred to as *server*) to opportunely update the rewards and select the goal point of each agent. Since the server can manage one reward matrix at a time, it is asynchronously handled by the various agents, with a priority approach: assuming

to have a system of  $M > 1$  agents, taking two general agents  $i$  and  $j$ , which request the server at the same time, the goal of  $i$  is processed before  $j$ 's if  $i < j$ .

Moreover, the server also stores the already assigned locations, to avoid reusing them. Indeed, to explore the biggest possible area of the environment, the goals for the agents need to be spread. To foster this sparsity, since there are many agents, we decided to update the reward function using Algorithm 5 and Equations 6-8, where  $d$  is the distance between the chosen goal and all other goal points.

$$K = \frac{\text{max reward in matrix}}{\text{number of already chosen points}} \quad (6)$$

$$k = \frac{K}{d^2} \quad (7)$$

$$R_{new} = R_{old} - k \quad (8)$$

It may be observed (Equation 8) how  $k$  represents a subtracting factor for the Reward matrix elements, updated when a target goal for one agent is selected. Since  $k$  is inversely dependent on the distance computed between the last chosen goal and the considered frontier point (Equation 7), the closer the point is closer to the already chosen goal, the higher will  $k$ , decreasing the probability that the point will be chosen as the next goal, thus achieving the task of spreading the goals in the environment.

The complete procedure for the selection of points (goals) is described in Algorithm 4, also including the relative function to update rewards when a goal is selected, described in Algorithm 5.

---

**Algorithm 4** Select Points

---

```

1: function  $sel_{pts}(PRewards, N_{goals})$ 
2:    $goals \leftarrow \{\}$ 
3:    $Mat \leftarrow$  Equation 5 using  $PRewards$  and  $N_{goals}$ 
4:   if  $Mat \neq \{\}$  then
5:      $p \leftarrow \text{Point2D}()$ 
6:     if  $cho_{cords} \neq \{\}$  then
7:        $Mat \leftarrow \text{upd\_rewards}(cho_{cords}, Mat)$ 
8:     end if
9:      $MaxRew_{ID} \leftarrow$  get maximum reward index in  $Mat$ 
10:     $p.x, p.y \leftarrow$  x,y value in  $Mat$  at  $MaxRew_{ID}$ 
11:    for  $pt \in cho_{cords}$  do
12:      if  $pt.x, pt.y = p.x, p.y$  then
13:         $Mat[MaxRew_{ID}, 0] \leftarrow -\infty$ 
14:         $MaxRew_{ID} \leftarrow$  get maximum reward index in  $Mat$ 
15:         $p.x, p.y \leftarrow$  x,y value at  $MaxRew_{ID}$ 
16:      end if
17:    end for
18:     $cho_{cords} \leftarrow p$ 
19:     $goals \leftarrow p$ 
20:  end if
21:  return  $goals$ 
22: end function

```

---

Algorithm 4 takes as input a list of points along with their rewards  $PRewards = \{r_1, x_1, y_1, \dots, r_N, x_N, y_N\}$  (computed with Equation 5, line 3), and updates the  $R_m$  matrix using Algorithm 5 (line 7), which first checks whether the frontier corresponds with the already selected goal, discarding the point in this case, and then updates the reward as described in Equations 6-8. The goal corresponding to the higher reward for the current agent, updated with the described policies, is eventually passed back to the agent.

The choice of the parameter  $K$  (Equation 6) is mainly motivating by two reasons:



---

**Algorithm 5** Update Rewards

---

```
1: function upd_rewards(cho_cords, Mat)
2:   MaxRew_val  $\leftarrow$  max. reward in Mat
3:   K  $\leftarrow$  Equation 6
4:   for c  $\in$  cho_cords & g  $\in$  Mat do
5:     if cx,y = gx,y then
6:       Mat[g] =  $-\infty$ 
7:     end if
8:     if Mat[g]  $\neq -\infty$  then ▷ compute distance from chosen goals
9:       d2  $\leftarrow \sqrt{(c_x - g_x)^2 + (c_y - g_y)^2}$ 
10:      if d2  $\neq 0$  then
11:        Mat[g]  $\leftarrow$  Equation 8
12:      else
13:        Mat[g] =  $-\infty$ 
14:      end if
15:    end if
16:  end for
17:  return Mat
18: end function
```

---

- the term `max_reward in matrix` allows for scaling *K* concerning the Reward Matrix of each single agent, normalizing the subtractive factor;
- the term `number of already chosen points` allows for distributing the reward update also taking into account the number of already selected points. Indeed, when the number of targets already explored becomes significant, each point will only receive a smaller portion of the total reward, resulting in a more limited effect of the subtractive parameter.

As described before, agents are managed asynchronously with a priority approach. The priority assigned to robots can lead to having one or more robots with low priority being stuck because they are always prioritized by higher-priority agents. To avoid this issue, the server also takes into account the number of requests not related to each agent. Once this number exceeds a certain predefined threshold, the corresponding agent will be associated with the higher priority. This approach will avoid having robots stuck, distributing goals more uniformly and is more effective than synchronous approach presented in our previous work [35].

## 4. Experimental Evaluation

### 4.1. Simulation Environment

To evaluate the proposed approach, simulations were performed with the simulation environment Gazebo on a PC with an Intel Core i7<sup>®</sup> (32GB RAM) and NVIDIA RTX 1000 GPU, equipped with Ubuntu 20.04 and ROS Noetic. Practically, a team of RosBots 2, equipped with lidar sensors were deployed in a modified version of the Willow Garage (W.G)<sup>4</sup> environment and of the AWS Hospital<sup>1</sup>, with area of 2071 and 1243  $m^2$  respectively.

Since our proposed approach aims at environment exploration while working on minimum frontier points with efficient AC-SLAM, we decided to use the following performance metrics:

- *percentage of map coverage*, to quantify the evolution of the covered map concerning the ground truth map;
- *number of frontier points*, to measure the average points reduction (corresponding to a decreased computational cost) achieved with the method described in Section 3.2.

---

<sup>4</sup><https://github.com/argp/Gazebo/>

<sup>1</sup><https://github.com/aws-robotics/aws-robomaker-hospital-world>

Figure 4 shows the resultant Occupancy Grid map along with the pose graphs of 3 agents in the AWS Hospital environment, considering 30 minutes of exploration time. We can observe that the proposed method provides an accurate map with 80% coverage while maintaining good SLAM accuracy. Figure 5 shows the resulting individual pose graphs from Open Karto SLAM, also indicating the loop closures performed by robots, which helps in reducing uncertainty.

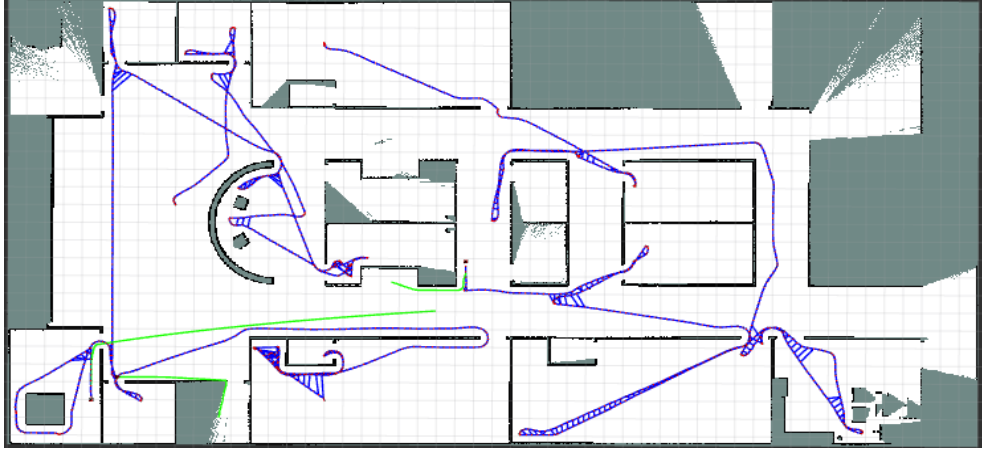


Figure 4: AWS Modified Hospital with 3 robots.

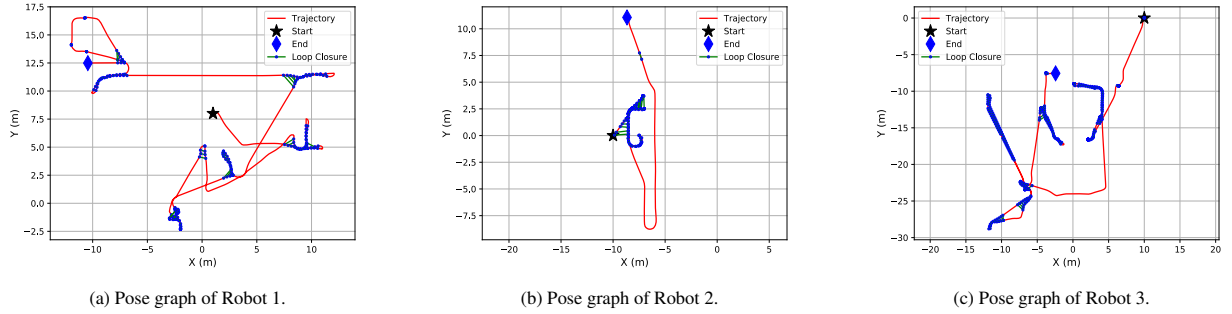


Figure 5: Resulting pose graphs of individual robots.

Figure 6a shows the results of 4 simulations (S1 to S4) using 2 and 3 robots, with and without the proposed utility function, again related to 30 minutes of exploration time, in the Willow Garage environment. In this scenario, we compared our proposed approach (designed as 'our') with the one using the utility function proposed by [5], as shown in Equation 3 (hereinafter referred as 'MAGS').

We can observe that with our approach (S2, S4) we manage to get 11% and 8% more area covered as compared to MAGS (S1, S3) respectively. This implies an area of  $228m^2$  and  $166m^2$  covered. As far as dealing with the computational complexity, i.e., in terms of reducing the number of processed frontier points, Figure 6b provides an insight into how the number of points used is reduced. We can deduce that using the methods in Section 3.2 and setting  $PER\_UNK = 60\%$ ,  $RAD = 1m$  we manage to drastically reduce the average number of points processed from 31 to 6 for S1 (81%), 37 to 7 for S2 (82%), 58 to 9 for S3 (85%), and 48 to 2 for S4 (96%) respectively, also exploring the environment more efficiently. This reduction in points is directly related to the computational complexity, as fewer points require computing the utility function with lesser frequency, hence accelerating the overall performance of the proposed system.

The same comparison has been carried out in the smaller AWS environment, with a simulation time of 25 minutes. Figure 7 shows the area coverage and points reduction with 'our' (S2, S4) and 'MAGS' (S1, S3) approaches. We can

observe that with the proposed approach (S2, S4) we managed to get a higher percentage (3% - 9%) of the area covered. This implies an increased coverage area between  $37m^2$  and  $112m^2$ . Since the AWS Hospital environment is much smaller than the Willow Garage one, results related to map coverage are quite high for both MAGS and our approach, but the small increase in coverage seems to confirm the effectiveness of our approach. Also in this case, the usage of the *Filtering and Classification* method described in Section 3.2 leads to a meaningful reduction in the number of points processed from 36 to 1 for S1 (98%), 29 to 4 for S2 (87%), 43 to 1 for S3 (98%), and 76 to 0 (no new points detected) for S4 respectively. The average values are smaller compared to those in Figure 6b (1.5 vs 6) since also the environment is smaller than before. Hence, the system is saturated with an average coverage of 80%, and no further exploration and coverage task is required.

The above-mentioned simulation results indicate the efficiency of our approach as compared to the state-of-the-art methods. To further evaluate the methodology, we performed tests with a team of ground robots in a real environment, whose results are presented in the following section.

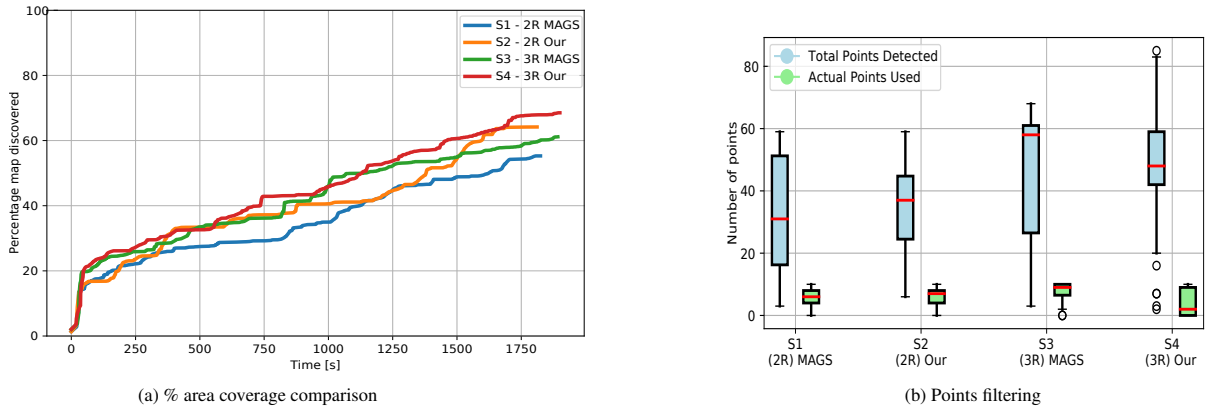


Figure 6: Willow Garage (W.G) % area coverage and points reduction comparison

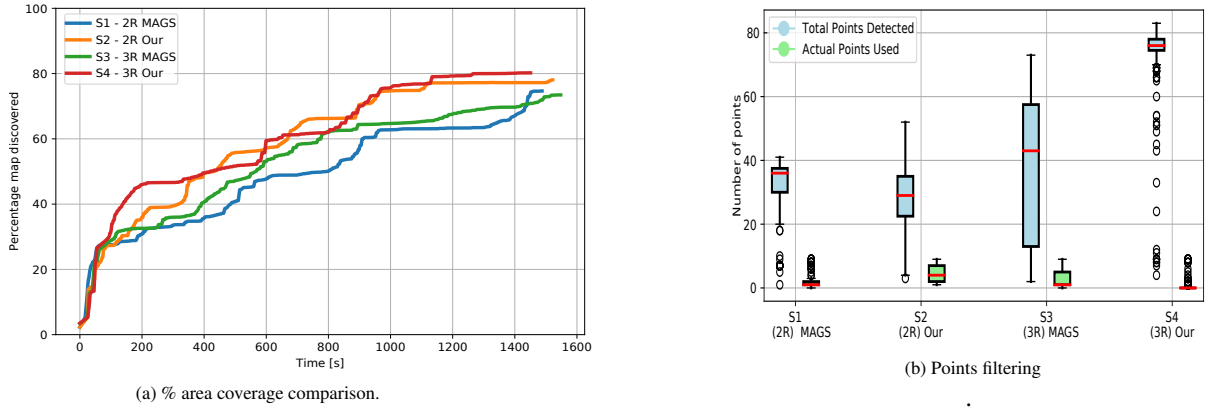


Figure 7: AWS Hospital % area coverage and points reduction comparison.

#### 4.2. Real Environment

Experiments in a real environment were performed using two ROSBot 2R robots<sup>5</sup> with RPLidar A2 (Figure 8a) with ROS on Ubuntu 20.04.6 (LTS). The robots are equipped with an Intel Xeon® W-2235 CPU 3.80GHz x 12, with 64Gb RAM and Nvidia Quadro RTX 4000 GPU. The environment consists of a room and two corridors measuring  $81m^2$  in total as shown in Figure 8b. Figure 8c shows the resultant Occupancy Grid map along with SLAM pose graphs, using the proposed approach with a team composed of two robots (red circles).

Figure 9a shows the percentage of maps discovered over time. As for simulation results, we compared the proposed utility function with the 'MAGS' one in eight experiments, considering an exploration time of 2 minutes. It can be shown that the proposed approach achieves a coverage of 98.85%, higher than the coverage percentage achieved with MAGS (94.25%). This implies a higher portion of map covered with the proposed approach (4.6%) and hence proves the effectiveness of the proposed method.

Figure 9b compares the number of points processed and detected in the four experiments. We can observe a significant reduction in the number of used points, from 6 to 5 for Exp 1 (17%), 7 to 3 for Exp 2 (58%), 3 to 2 for Exp 3 (34%), and 6 to 2 for Exp 4 (67%), resulting again in a reduction of the computational load.

Since the area of the experimental environment is much smaller, the exploration time was limited to only 2 minutes. Still, the increase of the map coverage (4.6%) was similar to the one achieved within the simulation (3% - 11%). The maximum number of points detected and processed is smaller concerning the simulation results, with an average reduction in the frontier points used equal to 44%.



Figure 8: Robot and experimental environment used.

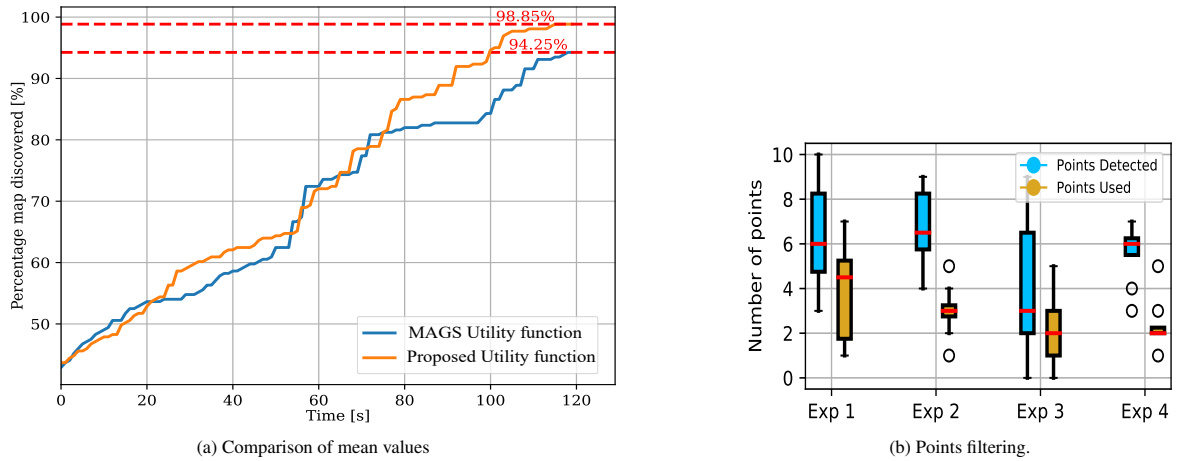


Figure 9: (9a) Comparison of mean values of map discovered with and without the proposed utility function. (9b) Total points detected vs the actual points used.

<sup>5</sup><https://husarion.com/manuals/rosbot/>.

## 5. Conclusion

In this article, we presented a multi-robot collaborative active SLAM framework for an environment exploration task. The proposed framework provides a utility function that incorporates the SLAM uncertainty and path entropy for the efficient selection of goal frontier candidates. We also propose an efficient frontier filtering method that encourages sparsity while working on a reduced number of frontier candidates, hence providing a less computationally expensive solution. The implementation exploits a ROS-based client-server paradigm in a modular software architecture.

Through various simulation results on publicly available environments and experiments in a real environment, we have proven the usefulness and applicability of our method as compared to selected state-of-the-art approaches and manage to achieve an accumulative 31% more coverage. In the future, we plan to extend our approach to visual AC-SLAM using heterogeneous robots to exploit the visual features and viewpoint changes of the environment.

## Acknowledgement

This work was carried out in the framework of the NExT Senior Talent Chair DeepCoSLAM, which was funded by the French Government, through the program Investments for the Future managed by the National Agency for Research ANR-16-IDEX-0007, and with the support of Région Pays de la Loire and Nantes Métropole. This research was also supported by the DIONISO project (progetto SCN\_00320-INVITALIA), which is funded by the Italian Government.

## References

- [1] Pham, V. C., Juang, J. C. (2011). An Improved Active SLAM Algorithm for Multi-robot Exploration . SICE Annual Conference 2011, 1660–1665.
- [2] Stachniss, C., Grisetti, G., Burgard, W. Information Gain-Based Exploration Using Rao-Blackwellized Particle Filters. In Proceedings of the Robotics: Science and Systems I; Robotics: Science and Systems Foundation, June 8 2005.
- [3] Qin, H., Meng, Z., Meng, W., Chen, X., Sun, H., Lin, F., , Ang, M. H. (2019). Autonomous exploration and mapping system using heterogeneous UAVs and UGVs in GPS-denied environments. IEEE Transactions on Vehicular Technology, 68(2), 1339–1350.
- [4] Meng, Z., Sun, H., Qin, H., Chen, Z., Zhou, C., Ang, M. H. (2017). Intelligent robotic system for autonomous exploration and active slam in unknown environments. SII.
- [5] Placed, J.A., Castellanos, J.A. Fast Autonomous Robotic Exploration Using the Underlying Graph Structure. (2021) IROS, Prague, Czech Republic, September 27 2021, pp. 6672–6679.
- [6] Yamauchi, B. A Frontier-Based Approach for Autonomous Exploration. (1997). CIRA'97. Monterey, CA, USA, 1997; pp. 146–151.
- [7] J. Du, L. Carlone, M. Kaouk Ng, B. Bona and M. Indri, "A comparative study on active SLAM and autonomous exploration with Particle Filters," 2011 IEEE/ASME AIM, Budapest, Hungary, pp. 916-923.
- [8] Brian J. Julian, Sertac Karaman, and Daniela Rus. "On mutual information-based control of range sensing robots for mapping applications". 2013 IROS, pp. 5156–5163.
- [9] Shi Bai et al. "Information-theoretic exploration with Bayesian optimization". 2016 IROS. pp. 1816–1822.
- [10] Shannon, C. E. (1948). A mathematical theory of communication. The bell system technical journal, 27, 623–656.
- [11] A. Papadimitriou, Foundations of optimum experimental design. Springer, 1996, vol. 14.
- [12] Dijkstra EW. A note on two problems in connexion with graphs. Numerische mathematik. 1959;1(1):269–71.
- [13] Carrillo, H., Reid, I., Castellanos, J. A. (2012, May). On the comparison of uncertainty criteria for active SLAM. In 2012 IEEE International Conference on Robotics and Automation: pp. 2080-2087.
- [14] Indelman, V. (2018). Towards cooperative multi-robot belief space planning in unknown environments. Springer Proceedings in Advanced Robotics, 441–457.
- [15] Ossenkopf, M., Castro, G., Pessacq, F., Geihs, K., & De Cristoforis, P. (2019). Long-Horizon Active Slam system for multi-agent coordinated exploration. EECR.
- [16] Kontitsis, M., Theodorou, E. A., & Todorov, E. (2013). Multi-robot active slam with relative entropy optimization. 2013 American Control Conference.
- [17] Placed, J.A.; Castellanos, J.A. A Deep Reinforcement Learning Approach for Active SLAM. Applied Sciences 2020, 10, 8386.
- [18] Pei, Z., Piao, S., Souidi, M., Qadir, M., & Li, G. (2018). Slam for humanoid multi-robot active cooperation based on relative observation. Sustainability, 10(8), 2946.
- [19] Placed, J. A., Strader, J., Carrillo, H., Atanasov, N., Indelman, V., Carlone, L., Castellanos, J. A. (2023). A survey on active simultaneous localization and mapping: State of the art and new frontiers. IEEE Transactions on Robotics (T-RO)
- [20] K. Naderi, J. Rajamäki, P. Härmäläinen, RT-RRT\*: a real-time path planning algorithm based on RRT\*, 8th ACM, Paris France, 2015: pp. 113–118.
- [21] Indelman, V. (2015). Towards multi-robot active collaborative state estimation via belief space planning. 2015 IEEE/RSJ International Conference on Intelligent Robots and Systems (IROS).
- [22] Chen, Y., Zhao, L., Lee, K. M., Yoo, C., Huang, S., Fitch, R. (2020). Broadcast your weaknesses: cooperative active pose-graph slam for multiple robots. IEEE Robotics and Automation Letters, 5(2), 2200–2207.

- [23] Li, J., Cheng, Y., Zhou, J., Chen, J., Liu, Z., Hu, S., Leung, V. C. (2022). Energy-efficient ground traversability mapping based on UAV-UGV collaborative system. *IEEE Transactions on Green Communications and Networking*, 6(1), 69–78.
- [24] Fox, D.; Burgard, W.; Thrun, S. Active Markov Localization for Mobile Robots. *Robotics and Autonomous Systems* 1998, 25, 195–207.
- [25] N. Mohamad Yatim, N. Buniyamin, Particle filter in simultaneous localization and mapping (SLAM) using differential drive mobile robot, *Jurnal Teknologi*. 77 (2015).
- [26] Arvanitakis, I., Tzes, A. (2017). Collaborative mapping and navigation for a mobile robot swarm. 2017 25th Mediterranean Conference on Control and Automation (MED).
- [27] Pham, V. C., Juang, J. C. (2013). A multi-robot, cooperative, and active SLAM algorithm for exploration. *International Journal of Innovative Computing, Information and Control*, 9(6), 2567–2583.
- [28] Batinović, A., Oršulić, J., Petrović, T., Bogdan, S. Decentralized Strategy for Cooperative Multi-Robot Exploration and Mapping. *IFAC-PapersOnLine* 2020, 53, 9682–9687.
- [29] H. W. Kuhn, 'The Hungarian method for the assignment problem', (1955) *Naval Research Logistics*, vol. 2, no. 1–2, pp. 83–97.
- [30] Jadhav, N., Behari, M., Wood, R., Gil, S. Multi-Robot Exploration without Explicit Information Exchange.
- [31] Khosoussi, K., Huang, S., Dissanayake, G. Novel Insights into the Impact of Graph Structure on SLAM. (2014) *IROS*, Chicago, IL, USA, pp. 2707–2714.
- [32] Khosoussi, K.; Giamou, M.; Sukhatme, G.S.; Huang, S.; Dissanayake, G.; How, J.P. Reliable Graphs for SLAM. *The International Journal of Robotics Research* 2019, 38, 260–298.
- [33] Fox, D.; Burgard, W.; Thrun, S. The Dynamic Window Approach to Collision Avoidance. *IEEE Robot. Automat. Mag.* 1997, 4, 23–33.
- [34] Kuzmin, Y. P., Bresenham's Line Generation Algorithm with Built-in Clipping. (1995). *Comput. Graph. Forum* 14, no. 5 : 275-280.
- [35] Maragliano, M., Ahmed, M.F., Recchiuto, C.T., Sgorbissa, A. and Fremont, V., 2023. Collaborative Active SLAM: Synchronous and Asynchronous Coordination Among Agents. *arXiv preprint arXiv:2310.01967*.